Research Paper

Sema3f Protects Against Subretinal Neovascularization In Vivo

Ye Sun [a], Raffael Liegl [a], Yan Gong [a], Anima Bühler [b], Bertan Cakir [b], Steven S. Meng [a], Samuel B. Burnim [a], Chi-Hsiu Liu [a], Tristan Reuer [b], Peipei Zhang [b], Johanna M. Walz [b], Franziska Ludwig [b], Clemens Lange [b], Hansjürgen Agostini [b], Daniel Böhringer [b], Günther Schlunck [b], Lois E.H. Smith [a], Andreas Stahl [b,*]

[a] Department of Ophthalmology, Harvard Medical School, Boston Children's Hospital, 300 Longwood Ave, Boston, MA 02115, USA
[b] Eye Center, Medical Center, Faculty of Medicine, University of Freiburg, Killianstrasse 5, 79106 Freiburg, Germany

ARTICLE INFO

ABSTRACT

Pathological neovascularization of the outer retina is the hallmark of neovascular age-related macular degeneration (nAMD). Building on our previous observations that semaphorin 3F (Sema3f) is expressed in the outer retina and demonstrates anti-angiogenic potential, we have investigated whether Sema3f can be used to protect against subretinal neovascularization in two mouse models. Both in the very low-density lipid-receptor knockout ($Vldlr^{-/-}$) model of spontaneous subretinal neovascularization as well as in the mouse model of laser-induced choroidal neovascularization (CNV), we found protective effects of Sema3f against the formation of pathologic neovascularization. In the $Vldlr^{-/-}$ model, AAV-induced overexpression of Sema3f reduced the size of pathologic neovascularization by 56%. In the laser-induced CNV model, intravitreally injected Sema3f reduced pathologic neovascularization by 30%. Combined, these results provide the first evidence from two distinct in vivo models for a use of Sema3f in protecting the outer retina against subretinal neovascularization.

© 2017 The Authors. Published by Elsevier B.V. This is an open access article under the CC BY-NC-ND license (http://creativecommons.org/licenses/by-nc-nd/4.0/).

1. Introduction

Age-related macular degeneration (AMD) is one of the leading causes of visual impairment and legal blindness in industrialized countries (Bressler, 2004; Finger et al., 2011). Especially the neovascular form of AMD (nAMD) can lead to substantial vision loss within months after onset if left untreated. Anti-vascular endothelial growth factor (VEGF) therapy introduced in 2006 can slow down disease progression and restore vision. However, long term clinical data demonstrate that despite continuous anti-VEGF therapy up to one third of patients will lose more than three lines of visual acuity over 5–7 years despite continuous anti-VEGF therapy (Wecker et al., 2016; Rofagha et al., 2013). In addition, the CATT study provided evidence for a continuous growth of the subretinal neovascular lesion area in AMD patients despite anti-VEGF therapy (Comparison of Age-related Macular Degeneration Treatments Trials Research et al., 2016). These data from clinical long-term studies clearly demonstrate the need for novel treatment approaches that are additive or supplementary to anti-VEGF treatment in nAMD.

Variation in patient responses to anti-VEGF therapy has been seen in clinical trials. One of the reasons why some patients do not respond to anti-VEGF therapy may be that nAMD subtypes differ in their response to anti-VEGF treatment (Gulat-Marnay et al., 1989; Sulzbacher et al., 2017; Ying et al., 2013). Retinal angiomatous proliferations (RAP) for example are lesions that originate from the deep retinal vasculature and progress towards the retinal pigment epithelium (RPE) to form subretinal neovascular membranes. This is different from the classic choroidal neovascularization (CNV) phenotype in nAMD with subretinal neovascularization originating from the choroid, not the retinal vasculature. In both instances, however, the end result is similar: the normally avascular outer retinal space becomes compromised by invading pathological blood vessels.

Semaphorins, also known as collapsins, were first identified as a family of genes encoding guidance molecules for the embryologic development of the nervous system (Gaur et al., 2009; Luo et al., 1993). The Semaphorin class 3 consists of seven soluble proteins of ~100 kDa (designated by the letters a–g), which are secreted by cells of multiple lineages, including epithelial cells, neurons, and specific tumor cells (Gaur et al., 2009). We have previously demonstrated that Sema3f is physiologically expressed in the outer retina while Sema3a is predominantly induced in the inner retina under hypoxic conditions (Buehler et al., 2013). We and others have also demonstrated an angiomodulatory role for semaphorins and their neuropilin (Nrp) and plexin receptors

* Corresponding author at: Eye Center, Medical Center, Faculty of Medicine, University of Freiburg, Killianstrasse 5, 79106 Freiburg, Germany.
E-mail address: andreas.stahl@uniklinik-freiburg.de (A. Stahl).

(Fukushima et al., 2011; Joyal et al., 2011; Soker et al., 1998). In this study, we investigated whether modulation of Sema3f in the outer retina alters the formation of pathological subretinal neovascularization in two different in vivo models.

The very low-density lipoprotein receptor knockout mouse ($Vldlr^{-/-}$) is an established model to study the development of spontaneous subretinal neovascular lesions originating from the deep retinal vascular plexus. These lesions are comparable to RAP in human patients (Grossniklaus et al., 2010; Heckenlively et al., 2003). Interestingly, we found in this study that $Vldlr^{-/-}$ retinas have reduced expression levels of Sema3f. Our results show that restoring Sema3f in these mice using an AAV approach significantly reduces both the number and size of subretinal neovascular lesions. In our second in vivo model, laser-induced CNV membranes originate from the choroidal circulation and thus resemble classic CNVs from human patients with nAMD. Our results show that in this model, the intravitreal injection of recombinant Sema3f protein significantly reduces the size of subretinal neovascular membranes following laser photocoagulation.

Combined, these data provide evidence that Sema3f levels can be modulated to protect the physiologically avascular outer retina from invasion by retinal as well as choroidal pathological neovascularization.

2. Materials and Methods

2.1. Animals

All animal studies were performed according to protocols approved by the Institutional Animal Care and Use Committee at the Boston Children's Hospital and the University of Freiburg Medical Center. $Vldlr^{+/-}$ (heterozygous) mice from Jackson Laboratory (Stock #002529) were bred to generate homozygous and wild type littermates. Wild type C57BL/6J mice from Charles River were used for laser CNV experiments.

2.2. Preparation of AAV2 Virus

AAV2 vector expressing mouse *Sema3f* cDNA (accession number: BC010976), which was cloned into a pAAV2-CMV-MCS vector driven by CMV promoter, was provided by SIRION Biotech (Cat. SB-S-AA-102-03). pAAV2-CMV-MCS vector without *Sema3f* cDNA was used as control. Recombinant AAV2 vectors were produced as previously described (Grieger et al., 2006; Vandenberghe et al., 2010). Briefly, AAV vector, rep/cap packaging plasmid, and adenoviral helper plasmid were mixed with polyethylenimine (Sigma) and transfected into HEK293T cells (catalog HCL4517; Thermo Scientific). Sixty hours after transfection, cells were harvested and the cell pellet was resuspended in virus buffer, followed by three cycles of freeze-thaw, and homogenization (Dounce). Cell debris was pelleted at 5000g for 20 min, and the supernatant was run on an iodixanol gradient. Recovered AAV vectors were washed three times with PBS using Amicon 100 K columns (EMD Millipore). Real-time PCR was used to determine genome titers of the recombinant AAV. This protocol also was used to prepare a control (AAV2-shControl). Viruses were diluted to various concentrations to test infection, and a concentration of approximately 2×10^{12} gc/ml was used for the experiments.

2.3. Subretinal Injection

Subretinal injection into $Vldlr^{-/-}$ P0 neonate eyes was performed as previously described (Matsuda and Cepko, 2004; Wang et al., 2014; Xiong et al., 2015) under a dissection microscope. P0 $Vldlr^{-/-}$ or wild type pups were anesthetized on ice for several minutes. The eyelid was prepped with Betadine, followed by water, then 70% ethanol using cotton swabs. A blade was used to gently cut open the eyelid. The pulled angled glass pipette was inserted into the subretinal space. Approximately 0.5 μl solution containing AAV2-control or AAV2-

Sema3f (2×10^{12} gc/ml) was introduced into the subretinal space and the injection volume was controlled through a micro-injector (FemtoJet, Eppendorf). After injection, curved forceps were used to slowly close the eyelid. Mice were placed on a circulating water blanket for warmth. The retinas were collected at P12 for PCR assay and P16 for whole mount analysis.

2.4. Laser-Induced CNV, Intravitreal Injection and Quantification

Argon laser treatment was performed as previously described (Ogata et al., 1997). In brief, animals were anesthetized and the pupils were dilated. Care was taken to use mice of the same age (6–8 weeks). The animals were positioned in front of an argon laser (VISULAS 532s, Zeiss). Settings for laser coagulation were spot size 100 μm, emission time 100 ms and laser energy 150 mW at emission wavelength 532 nm. Three laser burns were applied per eye. The development of a small white bubble as a sign for Bruch's membrane rupture was required for a sufficient laser burn (Tobe et al., 1998). Intravitreal injection was performed using a Hamilton syringe with 33G canula. Directly following laser, eyes were injected with 1 μl recombinant Sema3f (100 ng) or PBS control under microscopic visual control. On day 14 after laser photocoagulation, eyes were enucleated, fixed in 4% PFA for 30 min and then transferred to PBS. Choroid was dissected and the choroidal whole mount was mounted onto slides (Thermo Fisher Scientific) with the scleral side down in SlowFade anti-fade mounting medium (Life Technologies). After staining with isolectin IB4, CNV lesion size was quantified in a blinded fashion using the ImageJ software.

2.5. Quantification of Subretinal Neovascularization in the $Vldlr^{-/-}$ Model

Neovascularization analysis in the $Vldlr^{-/-}$ mice was performed as described (Stahl et al., 2009; Sun et al., 2015). The whole mounts of retinas from $Vldlr^{-/-}$ and wild type were stained with isolectin IB4 and imaged using Zeiss AxioObserver.Z1 microscope with a monochrome digital Zeiss camera AxioCam MRm focusing on the terminal end of lesions on the RPE layer (usually at P16), and individual images were merged to create one whole retinal image using automated merge function (mosaiX; Zeiss) in the software AxioVision 4.6.3.0 (Zeiss). ImageJ (National Institutes of Health, http://imagej.nih.gov/ij/) was used for quantification of subretinal neovascularization lesion number and area in $Vldlr^{-/-}$ retinas with designed plugins adapted from the method used to measure retinal neovascularization (SWIFT_NV) in the OIR model (Stahl et al., 2009) which use a user-designated threshold to mark lesion structures that clearly stand out from background fluorescence of normal vessels, and can automatically remove small artifacts by selecting objects with a minimum size of 100 pixels. Other larger artifacts such as occasional cellular debris or retinal periphery with hyperfluorescence can be manually excluded from quantification. Lesion numbers and areas were quantified with researchers masked to the identity of samples.

2.6. Confocal Imaging and 3D Reconstruction

Eyes were enucleated from $Vldlr^{-/-}$ mice at P16 and fixed in 4% paraformaldehyde followed by dissection and staining of the retinas with fluoresceinated isolectin IB4 (Invitrogen) to visualize subretinal neovascularization in whole mounted retinas. 3D reconstructed images were taken with confocal microscopy (Leica TCS SP2 AOBS) and z-stacks were 3D reconstructed using Volocity software (Perkin Elmer) as described (Sun et al., 2015).

2.7. Hematoxyilin and Eosin Staining

Slides were washed in xylene and dehydrated in absolute ethanol, 95% and 70% alcohol, PBS respectively. Harris hematoxylin solution

was applied for 8 min. The solution was rinsed off under running tap water and 1% acid (HCl) alcohol was placed on the samples for 30 s. Slides were washed with running tap water, then with 0.2% ammonia water for 1 min. Slides were then washed again with tap water and rinsed with 95% alcohol followed by a counterstain in eosin solution for 1 min. Dehydration in different concentrations of alcohol and fixation with xylene were eventually followed by mounting the specimen with a xylene based mounting medium.

2.8. Quantification of Retinal Thickness

H&E stained slides were imaged using a light microscope (Zeiss Axio ObserverZ1, Zeiss GmbH, Oberkochen, Germany) with a $10\times$ objective. The images were opened with ImageJ and a scale bar was placed in the original image as a reference. ONL thickness of each retina was measured using ImageJ's free hand line tool. 4–6 different retinas per group and 4–8 measurements per retina and structure (ONL) were recorded.

2.9. Fundus Fluorescein Angiography (FFA)

$Vldlr^{-/-}$ mice were anesthetized and injected intraperitoneally with fluorescein AK-FLUOR (Akorn, Lake Forest, IL) at 5 μg/g body weight. Fluorescent fundus images with dilated pupils were taken with a retinal-imaging microscope (Micron IV, Phoenix Research Laboratories) at 1, 5 and 10 min after fluorescein injection as described (Gong et al., 2015; Li et al., 2014).

2.10. RNA Isolation and Quantitative RT-PCR

Total RNA was extracted from mouse retinas using RNeasy kit (Qiagen) and reverse-transcribed with SuperScript® III Reverse Transcriptase (Thermo Fisher) to generate cDNA. Quantitative PCR was performed using a 7300 system (Applied Biosystems) with KAPA SYBR FAST qPCR Kits (Kapa Biosystems). Primer sequences from 5′ to 3′ for RT-PCR were as below and all primer efficencies were between 95 and 105%. Sema3f: TCG CGC ACA GGA TTA CAT CTT (Forward); ACC GGG AGT TGT ACT GAT CTG (Reverse); Nrp2: GCA GGT TTC TCT CTA CGC TAT G (Forward); CCT GGA GAT TCA ATG GTC CCA (Reverse); Vldlr: TCT CTT GCT CTT AGT GAT GG (Forward); CTT ACA ACT GAT ATT GCT GGG (Reverse).

2.11. Western Blot

A standard western blot protocol was used with minor modifications. Briefly, RIPA buffer (Pierce, 89900) was used to lyse cells. Proteinase inhibitor cocktail (Sigma, P8340) was added. Proteins were separated by electrophoresis using 4 to 12% NuPAGE Novex bis-Tris gels (Invitrogen, NP0321BOX). Mouse β-ACTIN (Sigma, A1978) antibody was used for control.

2.12. Statistics

Statistical analyses were performed with GraphPad Prism (v6.0) (GraphPad Software, Inc., San Diego, CA) and the results from the $Vldlr^{-/-}$ experiments are compared using the Mann Whitney test. Results from the laser-induced CNV experiments are presented as box plots and compared using the Wilcoxon rank sum test. A p value < 0.05 was considered to be statistically significant in all experiments.

3. Results

We have previously demonstrated that Sema3f is physiologically expressed in the outer retina (Buehler et al., 2013). In order to investigate whether Sema3f plays a role in regulating neovascularization in

the outer retina in vivo, we chose $Vldlr^{-/-}$ mice as a mouse model with RAP-like vascular phenotype. There are three retinal vascular layers (superficial, intermediate and deep) in the normal mouse retina (Fig. 1A, left). In the $Vldlr^{-/-}$ retina, neovascularization extends from the retinal vasculature into the normally avascular photoreceptor layer by postnatal day (P) 12 and reaches the RPE by P16 (Fig. 1A, right). These ectopic vessels reach the RPE and merge with choroidal vessels to form retinal-choroidal anastomoses and choroidal neovascularization around P90, violating the avascular privilege of the photoreceptor layer (Fig. 1B). To investigate whether loss of angiomodulatory Sema3f in the outer retina is associated with the formation of vascular lesions in the retinas of $Vldlr^{-/-}$ mice, we analyzed protein levels and mRNA expression of Sema3f (Fig. 1C, D). At all time points investigated, we found a reduction of Sema3f in the retina of $Vldlr^{-/-}$ mice. Neuropilin2 (Nrp2), the receptor for Sema3f, was also reduced in $Vldlr^{-/-}$ retinas (Fig. 1E). Using laser capture microdissection, Sema3f suppression was localized mainly to the outer nuclear layer (ONL) of $Vldlr^{-/-}$ mice at P12 (Fig. 1F). Since pathological vessels from the deep retinal plexus must pass through the ONL in order to reach the subretinal space, we further analyzed the effect of loss of Vldlr expression on immortalized retinal cells resembling cone photoreceptor cells. Confirming our in vivo results, we found that shRNA-mediated knock down of Vldlr in 661 W cells leads to a significant reduction of Sema3f (Fig. 1G).

To analyze whether loss of Sema3f contributes to the formation of subretinal neovascular lesions in $Vldlr^{-/-}$ mice, we designed two viral constructs using adeno-associated virus 2 (AAV2) vectors (Fig. 2A). The first construct (AAV2-GFP) was used for proof of principle experiments to test whether we could effectively target the outer retina (RPE and photoreceptors) with these constructs. The GFP expression was achieved with a transfection efficacy of about 75% (Figs. 2B and C). We found that a single subretinal injection of AAV2-GFP at postnatal day 0 (P0) induced GFP expression mainly in photoreceptor cells, but also to a minor extent in RPE, RGCs, INL and endothelial cells (Fig. 2C). Having established successful infection and gene expression in the outer retina using our viral construct, we used a Sema3f-expressing construct (AAV2-Sema3f) driven by CMV promoter to test whether restoring Sema3f expression to $Vldlr^{-/-}$ retinas would protect against subretinal neovascularization in these mice. pAAV2-CMV-MCS vector without Sema3f cDNA was used as control. Importantly, the AAV2-Sema3f construct does not carry the GFP gene to avoid possible immunologic responses of the retina or RPE to the xenogeneic GFP protein. After subretinal treatment of $Vldlr^{-/-}$ mice with the Sema3f-expressing viral construct, Sema3f expression was induced as well as expression of its receptor Nrp2, and the number and size of subretinal neovascular lesions were reduced by 40% and 56%, respectively (Fig. 2D–G).

We next investigated whether the protective effect of Sema3f against subretinal neovascularization could be reproduced using alternative in vivo approaches. First, by using in vivo fluorescein angiography we observed that AAV-induced overexpression of Sema3f not only reduced lesion size and number but also reduced leakage in $Vldlr^{-/-}$ mice (Fig. 3A). In addition, we evaluated whether AAV-induced Sema3f overexpression has long-term effects on retinal integrity in $Vldlr^{-/-}$ mice (Fig. 3B, C). These data demonstrate protection against retinal degeneration in 6-month old $Vldlr^{-/-}$ retinas, particularly in the ONL. We further examined the effect of Sema3f on subretinal neovascularization using an independent in vivo model by utilizing the mouse model of laser-induced CNV (Fig. 3D). In this model, CNV formation is induced by laser burns applied to Bruch's membrane and underlying choroid/RPE. Unlike the $Vldlr^{-/-}$ model, subretinal neovascularization in the laser-induced CNV model originates not from the retinal vessels, but from the choroidal circulation. Intravitreal injection of Sema3f protein in C57Bl6/J mice directly following laser treatment reduced the CNV size at day 14 by 30% compared with sham injected animals (Fig. 3E).
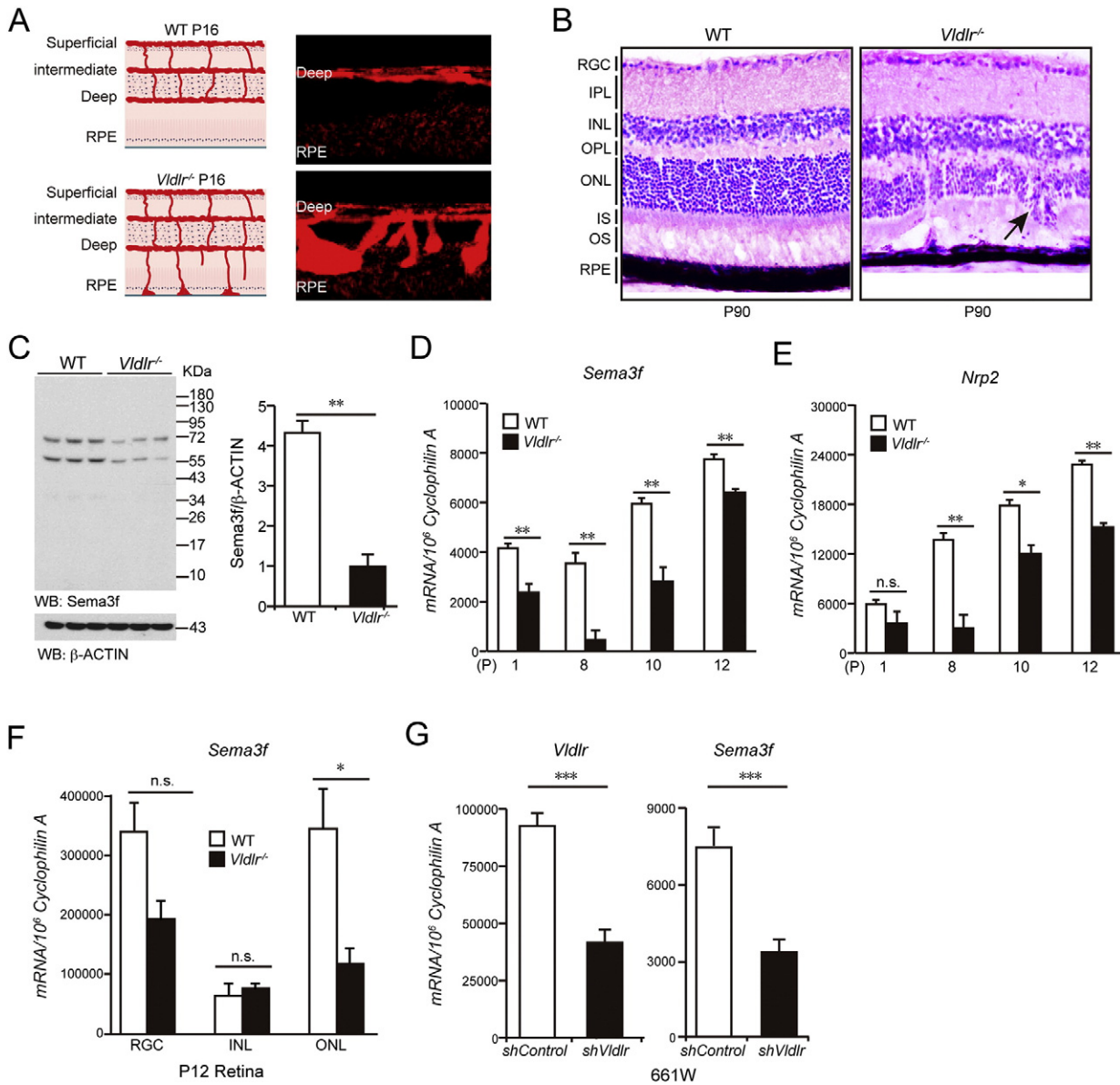
Fig. 1. Sema3f is suppressed in outer nuclear layer in *Vldlr* deficient retina. (A) Schematic illustration of spontaneous subretinal neovascularization in *Vldlr*$^{-/-}$ mice at P16. (B) H&E staining showing neovascularization and retinal layer disorganization in P90 *Vldlr*$^{-/-}$ retinas. Black arrow indicates the neovascularization. (C) Sema3f protein level is reduced in P12 *Vldlr*$^{-/-}$ retinas. (D, E) mRNA expression of *Sema3f* and its receptor, *Nrp2* are all markedly reduced in *Vldlr*$^{-/-}$ retinas compared with wild type (WT) littermate controls during retinal development. (F) *Sema3f* mRNA expression is mainly reduced in ONL, but not in RGC and INL in P12 *Vldlr*$^{-/-}$ retinas. (G) Reduced *Sema3f* mRNA level is confirmed in 661 W cells. *p < 0.05; **p < 0.01; ***p < 0.001; n.s., no statistical significance (n = 4–6).

4. Discussion

The aim of this study was to investigate whether Sema3f acts as an anti-angiogenic modulator suppressing formation of pathological neovascularization in the outer retina. Using two independent experimental approaches, we found potent anti-angiogenic activity of Sema3f in both, the *Vldlr*$^{-/-}$ model as well as the mouse model of laser-induced CNV. Importantly, these two models represent two different forms of subretinal neovascularization: in the *Vldlr*$^{-/-}$ mice, the pathological subretinal vessels originate from the deep retinal plexus and thus resemble RAP in humans, a subform of exudative AMD; the subretinal neovascularization in the laser-induced CNV model in contrast originates from the choroidal vascular plexus, thus resembling classic CNV lesions in human AMD.

Our two experimental approaches also differed with regard to the mode of Sema3f application. In the *Vldlr*$^{-/-}$ model, Sema3f was applied

via subretinal injection of a recombinant adeno-associated virus. For the laser-induced CNV model, we used an approach in which might be closer to clinical application by injecting Sema3f recombinant protein intravitreally. Both treatments led to a reduction of pathological neovascularization in the respective mouse models. Since intravitreal injection of anti-VEGF compounds is clinically well established (Ajlan et al., 2016; Meyer et al., 2016; Shao et al., 2016) and combinatory treatments are currently under investigation in clinical studies (Jaffe et al., 2016), intravitreal treatment with Sema3f alone or in combination with other compounds may be feasible for future treatment strategies in nAMD.

Any intravitreally injected substance must prove efficacy and safety. While our study was not designed as a preclinical safety study, we did not find any obvious structural changes after Sema3f treatment in either of the two in vivo models, which is not surprising given that *Sema3f* is physiologically expressed in the outer retina (Buehler et al., 2013). Our long-term follow-up experiments in *Vldlr*$^{-/-}$ mice showed even
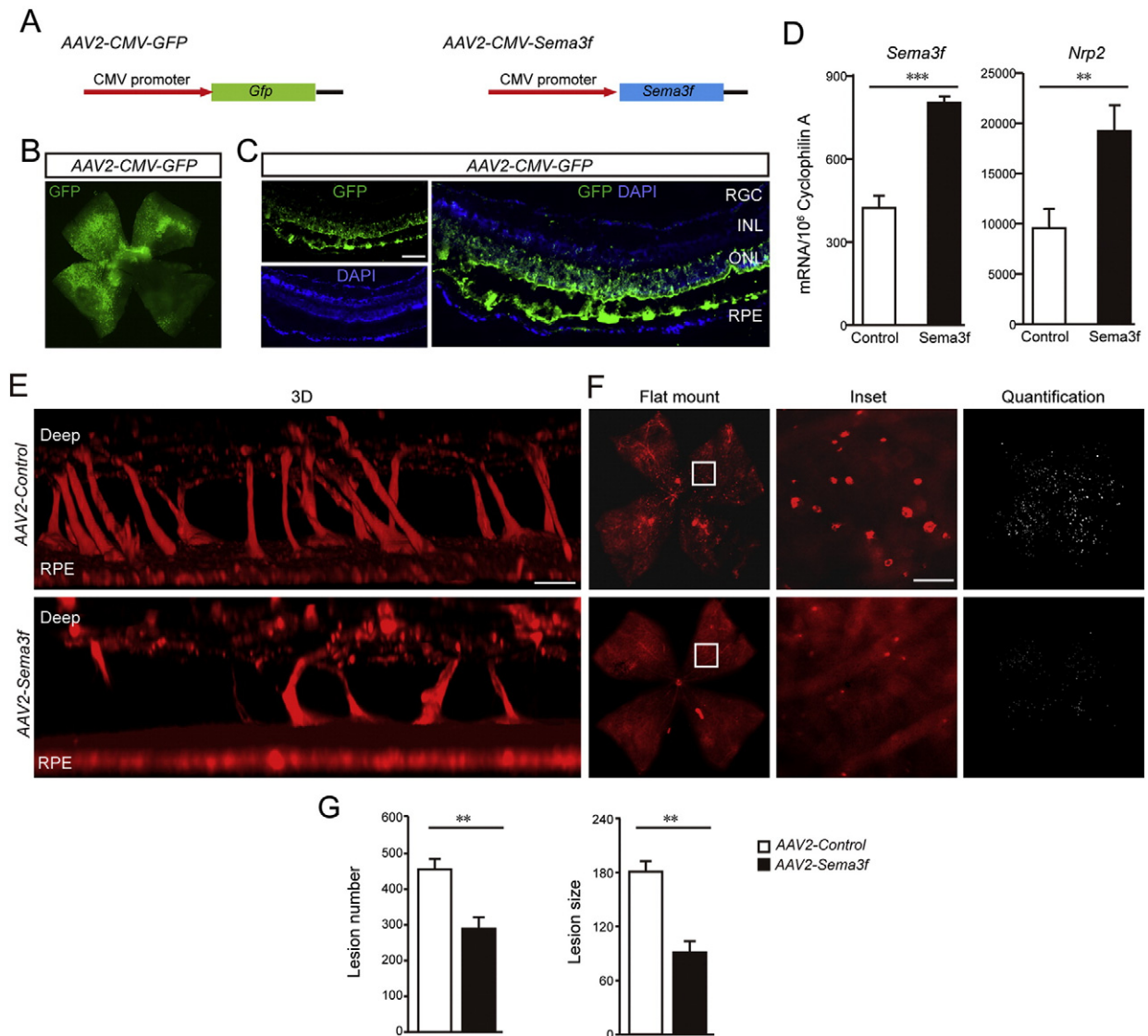
Fig. 2. AAV2-CMV-*Sema3f* suppresses subretinal neovascularization induced by *Vldlr* deficiency. (A) AAV2 constructs carrying *Sema3f* or *GFP* driven by CMV promoter. (B) Representative retinal flatmount image of a C57Bl6/J wild type animal showing that over 70% of the retina is successfully transfected by AAV2-CMV-GFP delivered by a single subretinal injection. (C) Representative cross section from a C57Bl6/J wild type treated by a single subretinal injection with AAV2-CMV-GFP showing efficient transfection. Green: GFP; blue: nuclear DAPI. Note that the dark band between ONL and RPE is due to artificial tissue separation during preparation. (D) Increased mRNA level of *Sema3f* is confirmed in AAV2-CMV-*Sema3f*-infected retinas compared with AAV2-CMV-Vector-infected retinas (n = 6). The mRNA level of *Nrp2* was induced in AAV2-CMV-*Sema3f*- infected retinas compared with AAV2-CMV-Vector-infected retinas (n = 6). (E–G) 3D reconstruction, representative images of flat-mounts and quantification of neovascular lesion number and size showing that AAV2-CMV-*Sema3f* suppresses subretinal pathological neovascularization in *Vldlr*$^{-/-}$ retinas at P16. Lesions on flat mount were highlighted (white) in F (right panel) and enlarged in inset. Scale bar, 500 μm for flatmount, 250 μm for inset, 1000 μm in 3B; 100 μm in 3C and D.

improved retinal integrity compared to control treated eyes, which may be a secondary benefit from reduced number and size of subretinal neovascular lesions.

In summary, these data provide to our knowledge the first proof of concept that Sema3f can be used to modulate pathological subretinal neovascularization. The protective effect of Sema3f was observed in two independent model systems and with two independent modes of application. The fact that Sema3f is physiologically expressed in the retina of both mice and humans (Buehler et al., 2013) renders Sema3f a promising target for treating pathological neovascularization formation in AMD.

Conflicts of Interest

There are no conflicts of interest.

Author Contributions

Y.S. and A.S. conceived and designed the study, analyzed the data and prepared all the figures. Y.S., A.S. and L.S. wrote the manuscript. Y.S., R.L., Y.G., A.B., B.C., S.M., S.B., C-H. L., T.R., P.Z., J.M.W., F.L. C.L. H.A., D.B. and G.S. performed the experiments, analyzed and/or interpreted data. All authors edited and approved the manuscript.
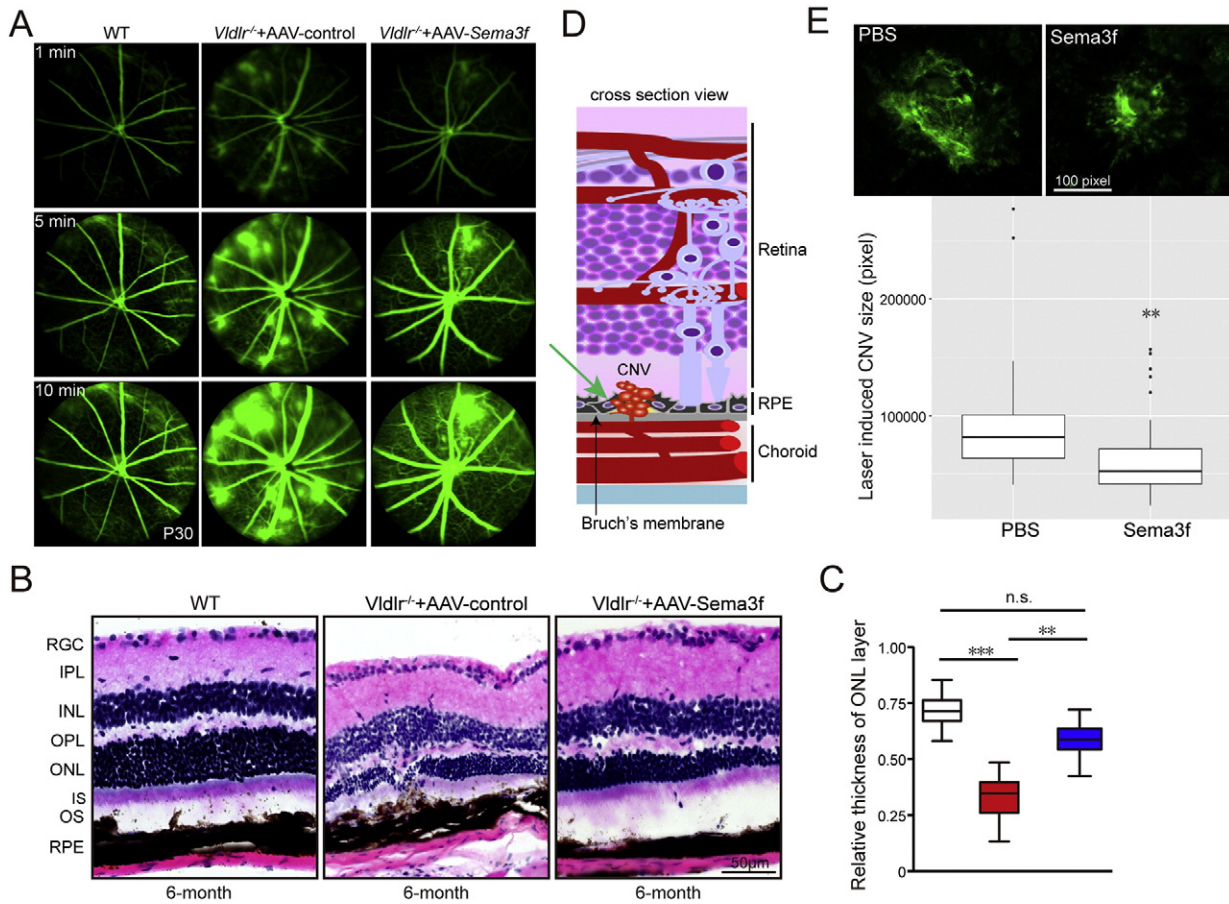
Fig. 3. AAV2-CMV-*Sema3f* or Sema3f recombinant protein protects against leakage from subretinal neovascularization, photoreceptor degeneration induced by *Vldlr* deficiency or laser-induced CNV. (A) Representative fluorescein angiography images from WT and *Vldlr*$^{-/-}$ treated with AAV2-control or AAV2-CMV-*Sema3f*. Images were taken 1, 5 and 10 min after intraperitoneal injection of fluorescent dye showing that AAV-CMV-*Sema3f* reduces neovascularization and prevents retinal vascular leakage induced by *Vldlr* deficiency (n = 6). (B, C) H&E staining and thickness quantification demonstrate that AAV2-CMV-*Sema3f* treatment prevents photoreceptor degeneration compared with 6-month old AAV2-CMV-Vector control treated mice (n = 26–31). (D) Schematic illustration of subretinal neovascularization originating from the choroidal vasculature in the laser-induced CNV mouse model. (E) Sema3f recombinant protein protects against laser-induced CNV compared with PBS treatment (n = 60–69 lesions from 23 to 26 eyes). *p < 0.05; **p < 0.01; ***p < 0.001; n.s., no statistical significance.

References

Ajlan, R.S., Silva, P.S., Sun, J.K., 2016. Vascular endothelial growth factor and diabetic retinal disease. Semin. Ophthalmol. 31, 40–48.

Bressler, N.M., 2004. Age-related macular degeneration is the leading cause of blindness. JAMA 291, 1900–1901.

Buehler, A., Sitaras, N., Favret, S., Bucher, F., Berger, S., Pielen, A., Joyal, J.S., Juan, A.M., Martin, G., Schlunck, G., et al., 2013. Semaphorin 3F forms an anti-angiogenic barrier in outer retina. FEBS Lett. 587, 1650–1655.

Comparison of Age-related Macular Degeneration Treatments Trials Research, G, Maguire, M.G., Martin, D.F., Ying, G.S., Jaffe, G.J., Daniel, E., Grunwald, J.E., Toth, C.A., Ferris 3rd, F.L., Fine, S.L., 2016. Five-year outcomes with anti-vascular endothelial growth factor treatment of neovascular age-related macular degeneration: the comparison of age-related macular degeneration treatments trials. Ophthalmology 123, 1751–1761.

Finger, R.P., Fimmers, R., Holz, F.G., Scholl, H.P., 2011. Prevalence and causes of registered blindness in the largest federal state of Germany. Br. J. Ophthalmol. 95, 1061–1067.

Fukushima, Y., Okada, M., Kataoka, H., Hirashima, M., Yoshida, Y., Mann, F., Gomi, F., Nishida, K., Nishikawa, S., Uemura, A., 2011. Sema3E-PlexinD1 signaling selectively suppresses disoriented angiogenesis in ischemic retinopathy in mice. J. Clin. Invest. 121, 1974–1985.

Gaur, P., Bielenberg, D.R., Samuel, S., Bose, D., Zhou, Y., Gray, M.J., Dallas, N.A., Fan, F., Xia, L., Lu, J., et al., 2009. Role of class 3 semaphorins and their receptors in tumor growth and angiogenesis. Clin. Cancer Res. 15, 6763–6770.

Gong, Y., Li, J., Sun, Y., Fu, Z., Liu, C.H., Evans, L., Tian, K., Saba, N., Fredrick, T., Morss, P., et al., 2015. Optimization of an image-guided laser-induced choroidal neovascularization model in mice. PLoS One 10, e0132643.

Grieger, J.C., Choi, V.W., Samulski, R.J., 2006. Production and characterization of adeno-associated viral vectors. Nat. Protoc. 1, 1412–1428.

Grossniklaus, H.E., Kang, S.J., Berglin, L., 2010. Animal models of choroidal and retinal neovascularization. Prog. Retin. Eye Res. 29, 500–519.

Gulat-Marnay, C., Lafitte, A., Arrang, J.M., Schwartz, J.C., 1989. Modulation of histamine release and synthesis in the brain mediated by alpha 2-adrenoceptors. J. Neurochem. 53, 513–518.

Heckenlively, J.R., Hawes, N.L., Friedlander, M., Nusinowitz, S., Hurd, R., Davisson, M., Chang, B., 2003. Mouse model of subretinal neovascularization with choroidal anastomosis. Retina 23, 518–522.

Jaffe, G.J., Eliott, D., Wells, J.A., Prenner, J.L., Papp, A., Patel, S., 2016. A phase 1 study of intravitreous E10030 in combination with ranibizumab in neovascular age-related macular degeneration. Ophthalmology 123, 78–85.

Joyal, J.S., Sitaras, N., Binet, F., Rivera, J.C., Stahl, A., Zaniolo, K., Shao, Z., Polosa, A., Zhu, T., Hamel, D., et al., 2011. Ischemic neurons prevent vascular regeneration of neural tissue by secreting semaphorin 3A. Blood 117, 6024–6035.

Li, J., Liu, C.H., Sun, Y., Gong, Y., Fu, Z., Evans, L.P., Tian, K.T., Juan, A.M., Hurst, C.G., Mammoto, A., et al., 2014. Endothelial TWIST1 promotes pathological ocular angiogenesis. Invest. Ophthalmol. Vis. Sci. 55, 8267–8277.

Luo, Y., Raible, D., Raper, J.A., 1993. Collapsin: a protein in brain that induces the collapse and paralysis of neuronal growth cones. Cell 75, 217–227.

Matsuda, T., Cepko, C.L., 2004. Electroporation and RNA interference in the rodent retina in vivo and in vitro. Proc. Natl. Acad. Sci. U. S. A. 101, 16–22.

Meyer, C.H., Krohne, T.U., Charbel Issa, P., Liu, Z., Holz, F.G., 2016. Routes for drug delivery to the eye and retina: intravitreal injections. Dev. Ophthalmol. 55, 63–70.

Ogata, N., Yamamoto, C., Miyashiro, M., Yamada, H., Matsushima, M., Uyama, M., 1997. Expression of transforming growth factor-beta mRNA in experimental choroidal neovascularization. Curr. Eye Res. 16, 9–18.

Rofagha, S., Bhisitkul, R.B., Boyer, D.S., Sadda, S.R., Zhang, K., Group, S.-U.S., 2013. Seven-year outcomes in ranibizumab-treated patients in ANCHOR, MARINA, and HORIZON: a multicenter cohort study (SEVEN-UP). Ophthalmology 120, 2292–2299.

Shao, J., Choudhary, M.M., Schachat, A.P., 2016. Neovascular age-related macular degeneration. Dev. Ophthalmol. 55, 125–136.

Soker, S., Takashima, S., Miao, H.Q., Neufeld, G., Klagsbrun, M., 1998. Neuropilin-1 is expressed by endothelial and tumor cells as an isoform-specific receptor for vascular endothelial growth factor. Cell 92, 735–745.

Stahl, A., Connor, K.M., Sapieha, P., Willett, K.L., Krah, N.M., Dennison, R.J., Chen, J., Guerin, K.I., Smith, L.E., 2009. Computer-aided quantification of retinal neovascularization. Angiogenesis 12, 297–301.

Sulzbacher, F., Pollreisz, A., Kaider, A., Kickinger, S., Sacu, S., Schmidt-Erfurth, U., Vienna Eye Study, C., Jan. 30, 2017. Identification and clinical role of choroidal neovascularization characteristics based on optical coherence tomography angiography. Acta Ophthalmol. http://dx.doi.org/10.1111/aos.13364.

Sun, Y., Liu, C.H., SanGiovanni, J.P., Evans, L.P., Tian, K.T., Zhang, B., Stahl, A., Pu, W.T., Kamenecka, T.M., Solt, L.A., et al., 2015. Nuclear receptor RORalpha regulates pathologic retinal angiogenesis by modulating SOCS3-dependent inflammation. Proc. Natl. Acad. Sci. U. S. A. 112, 10401–10406.

Tobe, T., Ortega, S., Luna, J.D., Ozaki, H., Okamoto, N., Derevjanik, N.L., Vinores, S.A., Basilico, C., Campochiaro, P.A., 1998. Targeted disruption of the FGF2 gene does not prevent choroidal neovascularization in a murine model. Am. J. Pathol. 153, 1641–1646.

Vandenberghe, L.H., Xiao, R., Lock, M., Lin, J., Korn, M., Wilson, J.M., 2010. Efficient serotype-dependent release of functional vector into the culture medium during adeno-associated virus manufacturing. Hum. Gene Ther. 21, 1251–1257.

Wang, S., Sengel, C., Emerson, M.M., Cepko, C.L., 2014. A gene regulatory network controls the binary fate decision of rod and bipolar cells in the vertebrate retina. Dev. Cell 30, 513–527.

Wecker, T., Ehlken, C., Buhler, A., Lange, C., Agostini, H., Bohringer, D., Stahl, A., 2016. Five-year visual acuity outcomes and injection patterns in patients with pro-re-nata treatments for AMD, DME, RVO and myopic CNV. Br. J. Ophthalmol. 101, 353–359.

Xiong, W., MacColl Garfinkel, A.E., Li, Y., Benowitz, L.I., Cepko, C.L., 2015. NRF2 promotes neuronal survival in neurodegeneration and acute nerve damage. J. Clin. Invest. 125, 1433–1445.

Ying, G.S., Huang, J., Maguire, M.G., Jaffe, G.J., Grunwald, J.E., Toth, C., Daniel, E., Klein, M., Pieramici, D., Wells, J., et al., 2013. Baseline predictors for one-year visual outcomes with ranibizumab or bevacizumab for neovascular age-related macular degeneration. Ophthalmology 120, 122–129.